Numerical Study of Developing Flow and Heat Transfer in Wavy Passages

K. M. Stone and S. P. Vanka

ACRC TR-104 August 1996

For additional information:

Air Conditioning and Refrigeration Center
University of Illinois
Mechanical & Industrial Engineering Dept.
1206 West Green Street
Urbana, IL 61801

(217) 333-3115

Prepared as part of ACRC Project 65
Investigation of Wavy Fins for Heat Transfer
Augmentation in Refrigeration/Air Conditioning Systems
A. M. Jacobi, T. A. Newell and S. P. Vanka, Principal Investigators

The Air Conditioning and Refrigeration Center was founded in 1988 with a grant from the estate of Richard W. Kritzer, the founder of Peerless of America Inc. A State of Illinois Technology Challenge Grant helped build the laboratory facilities. The ACRC receives continuing support from the Richard W. Kritzer Endowment and the National Science Foundation. The following organizations have also become sponsors of the Center.

Amana Refrigeration, Inc.
Brazeway, Inc.
Carrier Corporation
Caterpillar, Inc.
Dayton Thermal Products
Delphi Harrison Thermal Systems
Eaton Corporation
Ford Motor Company
Frigidaire Company
General Electric Company
Lennox International, Inc.
Modine Manufacturing Co.
Peerless of America, Inc.
Redwood Microsystems, Inc.
U. S. Army CERL
U. S. Environmental Protection Agency
Whirlpool Corporation

For additional information:

Air Conditioning & Refrigeration Center
Mechanical & Industrial Engineering Dept.
University of Illinois
1206 West Green Street
Urbana IL 61801

217 333 3115

NUMERICAL STUDY OF DEVELOPING FLOW AND HEAT TRANSFER IN WAVY PASSAGES

by Kevin Stone and S. Pratap Vanka

ABSTRACT

Developing flow in a wavy passage is analyzed using an accurate numerical scheme to solve the unsteady flow equations. Calculations are presented for a channel consisting of 14 waves. Systematic time-dependent simulations have been performed for Reynolds numbers (Re) ranging from 300 to 700. It is observed that the flow is steady in part of the channel and unsteady in the rest of the channel. As the Reynolds number is progressively increased, the unsteadiness is onset at a much earlier location, accompanied by increased overall heat transfer and friction coefficients.

NOMENCLATURE

D_h	Hydraulic diameter [m]
f	Friction factor
h	Heat transfer coefficient [W / m^2 - K]
H	Interwall spacing [m]
k	Thermal conductivity [W / m - K]
Nu	Nusselt number
p	Pressure [N / m^2]
Q	Volumetric flow rate [m^2 / s]
Re	Reynolds number Q / ν
t	Time [sec]
u	Cartesian velocity component in the x direction [m / s]
v	Cartesian velocity component in the y direction [m / s]
x	Cartesian coordinate
y	Cartesian coordinate

Greek Symbols

λ	Wavelength of the wavy wall [m]
ν	Kinematic molecular viscosity [m^2 / s]
θ	Dimensionless temperature
ρ	Density [kg / m^3]

Subscripts and Superscripts

avg	Spatially averaged quantity
m	Bulk mean quantity
max	Quantity evaluated at maximum cross-section

1. INTRODUCTION

In a previous study, Wang and Vanka (1995) analyzed heat transfer and fluid flow in a periodically fully-developed wavy passage. It was found that the flow field is steady until a Reynolds number (Re = Q/ν) of approximately 160, after which it becomes unsteady. The unsteadiness in the flow, resulting from the onset of Kelvin-Helmholtz type instabilities of the shear layers provides increased mixing of the core and near-wall fluids, thereby enhancing the rates of heat and mass transfer. Thus, wavy passages can be used as heat transfer enhancement devices in compact heat exchangers, when the flow rates and the passage dimensions are such that the flow transitions to a self-sustaining oscillatory state. In comparison with other techniques to enhance heat transfer, such as louvers, vortex generators, etc., wavy passages are easier to fabricate and may be attractive for other reasons as well.

The Reynolds number at which the flow becomes unsteady is usually low, as demonstrated in several numerical (*cf.* Sparrow and Prata, 1983; Guzmán and Amon, 1994) and experimental studies (*cf.* Mendes and Sparrow, 1984; Nishimura et al., 1984; Nishimura et al., 1986). However, numerical studies conducted so far have considered the flow to be periodic in the streamwise direction. By making this assumption, the computational domain could be restricted to just one wave of the passage, with imposition of the inflow and outflow variables. But such an assumption is only valid in the far region of a very long passage, and does not capture the entrance phenomena. In reality, most passages are short in length, and as a result, the characteristics observed for the periodic region may not be applicable. In particular, the assumption of periodicity in the streamwise direction imposes the condition of "absolute instability," whereas the flow may be "convectively unstable" at that particular Reynolds number. The implications can be profound; i.e. there can be significant differences in the Reynolds number where the flow becomes unsteady. Thus, the level of heat transfer enhancement that is expected when the flow is assumed to be unsteady may not be realized in practice.

Numerical studies of the developing region are far more cumbersome than for the fully-developed region. In order to understand the complete flow development, a long flow domain consisting of a number of wavy passages is necessary. Each wave must be accurately discretized to resolve the boundary layers on the walls. The time-integration must be carried out for much longer times, to investigate if some of the instability modes will grow. In the case of periodic conditions, the instabilities are recycled back to the inflow, and therefore, are made to grow faster if the flow is indeed unstable. Since the entrance effects are important in judging whether the candidate heat transfer passage is truly beneficial, a complete analysis of the channel length must be performed. Hence, in this paper we examine the developing region to determine the flow behavior as a function of the inlet Reynolds number, and as a function of streamwise location in a long wavy passage. It will be shown that at different Reynolds numbers, the transition occurs in different waves, with an averaged heat transfer enhancement lower than what is obtained in the periodic region. The present study also confirms the occurrence of "intermittent instability" experimentally observed in studies of Greiner, et al. (1990) for a passage with triangular grooves on one of the walls. This intermittent instability is very interesting from the viewpoint of nonlinear dynamics, and can be the subject of much fundamental study on the properties of the Navier-Stokes equations.

2. MATHEMATICAL FORMULATION

In the present study, the flow is considered to be two-dimensional with no variation in the spanwise direction. Therefore, the two-dimensional conservation equations are solved on a curvilinear orthogonal grid. The orthogonal mesh is generated by a general case of sequential mapping by solving a pair of elliptic partial differential equations.

The numerical integration of the equations is based on a two-step fractional step procedure with backward Euler differencing of the time derivative and Adams-Bashforth explicit differencing of the convection terms. The Crank-Nicolson implicit scheme is used for the diffusion terms.

The spatial discretization uses a collocated arrangement with the two Cartesian velocities and the pressure positioned at the centers of discrete finite volumes in the computational domain. The continuity equation is satisfied by the mass fluxes located at the cell faces. The pressure Poisson equation is solved using the conjugate gradient technique without preconditioning. Details of the procedure are similar to the study of Wang and Vanka (1995) and are available in that reference.

Figure 1 shows the flow domain for which the computations were performed. The passage includes fourteen periodic waves with the geometry and dimensions corresponding to the experiments of Nishimura, et al. (1984). It consists of two sinusoidal wavy walls that are placed with a mean spacing of 1.3 units. Each wave has a minimum height (H_{min}) of 0.6, a maximum height (H_{max}) of 2.0, and a wavelength (λ) of 2.8. Two straight sections with height H_{min} and length λ are attached at the entrance and exit of the computational domain.

At the inlet to the passage, the boundary condition was taken to be a uniform velocity distribution, whereas at the outlet, a zero-derivative boundary condition is applied.
Fourth order accuracy was used in the discretization of the derivatives. All of the calculations presented here were performed using an orthogonal curvilinear grid containing 64 x 64 internal cells over each wavelength. This translates to an overall grid of 1024 x 64 cells for the fourteen-wave channel. Grid refinement studies have shown that the 64 x 64 grid produces accurate results with a reasonable degree of computational efficiency.

Calculations were performed for Reynolds numbers ranging from 300 to 700. All of the simulations were run for a sufficiently long time so that the initial conditions were completely convected out of the passage, and had no effect on the final flow field. Local Nusselt numbers were calculated at the top wall using the relation $Nu = \frac{D_h \, \partial\theta / \partial n}{\theta_m}$, where the hydraulic diameter was taken to be the average height of the wavy passage. The average Nusselt number across a single wavelength could then be calculated by integrating the local values. Average friction factors were calculated by the relation $f = \frac{\Delta p}{\frac{1}{2}\rho u_{avg}^2}$, where Δp is the pressure difference across a single wavelength, and u_{avg} is the velocity prescribed uniformly at the inlet to the passage.

3. RESULTS AND DISCUSSION

Before performing the final set of calculations that are the subject of this paper, some calculations were performed using coarser grids, in order to determine how much the results of the calculations depend on: i) mesh density, and ii) the overall length of the wavy passage. First, calculations were performed using a 32 x 32 grid for each wave for flow through a passage

containing only eight waves, rather than fourteen. Simulations for this case were conducted for Reynolds numbers of 300, 400, 500, and 700. Next, numerical simulations were performed using a 64 x 32 grid for flow through a passage that had fourteen waves, and the results were compared with those obtained for the eight wave, coarse grid case described above.

Qualitatively, the results for these two sets of coarse grid calculations showed good agreement. For Re = 300 and Re = 400, the flow was completely steady throughout the entire channel in both cases, producing relatively trivial results. At Re = 500 and Re = 700, u-velocity time signals (discussed further in next section) revealed a transition to unsteadiness at a certain point within the bounds of the channels being investigated. For both Reynolds numbers, this transition occurred at the same position relative to the inlet regardless of the total length of the channel. Furthermore, the patterns of the time signals did not vary with the refinement of the grid. However, in order to ensure the highest possible degree of accuracy, a 64 x 64 grid per wave is employed for the results presented below.

Calculations were performed using a 64 x 64 mesh for each wavelength, for flow through a 14-wave passage, at Re = 300, 500, 600, 700. This provides a representative sampling of developing flow in a wavy passage in the regime where transition to an oscillatory state takes place. During each simulation, the instantaneous u-velocities were monitored to determine whether the flow was steady or unsteady at selected locations in the channel. These velocity "probes" were arbitrarily placed at a height of $0.75H_{max}$ in the tallest part of each wave.

Figure 2 shows the u-velocity time signal in wave 14 for Re = 300. At Re = 300, it is evident from the time signals that the flow becomes steady almost immediately after the initial conditions are convected out of the channel. The streamline plot in Figure 3 shows single trapped vortices in the cavities, and almost perfectly straight core flow. These are the expected patterns for steady flow in a wavy passage (Wang and Vanka, 1995). The coarse grid calculations revealed the same behavior at Re = 400, so in the interest of saving computer time, those calculations were not repeated using the finer mesh.

At Re = 500, however, the flow behavior becomes more interesting. Looking at the time signals for waves 8, 10, 12, and 14 in Figure 4(a)-4(d), one can see a unique pattern developing. For a certain period of time, the time signal does not fluctuate significantly, and the flow appears to be steady, resulting in a flow pattern that is similar to what is seen in Figure 3 for the Re = 300 case. Then, suddenly, large oscillations begin to appear, indicating that the flow is unsteady. The resulting flow pattern contains multiple vortices and divergent core flow, especially in the last two waves of the passage, as shown in Figure 5. This unsteady flow lasts for a certain amount of time, until the oscillations quickly die out, and the flow becomes steady again. After awhile, the pattern repeats itself. Thus, eight waves downstream and beyond, the flow displays intermittent unsteadiness. It is unsteady for some of the time and steady for the rest of the time. However, one can see from the time signals that the fluctuating sections become longer as we move downstream. The length of time that the flow is unsteady also increases. By the fourteenth wave, there are oscillations in the portion of the signal where the flow is completely steady in the upstream channels. Figure 6 shows the percentage of time that the flow is unsteady at Re = 500 plotted as a function of streamwise location. The flow is completely steady through the sixth wave downstream, but by the twelfth wave, the flow is unsteady almost 80% of the time. This is important, because heat transfer enhancement is not realized while the flow remains steady. This intermittent nature of flow was also observed in experiments of Greiner et al. (1990) in a channel with triangular grooves on one of the walls.

At Re = 600, the flow is oscillatory beginning at the fifth wave. It is completely unsteady downstream of this point, and the time signals in Figure 7 do not display the intermittent behavior seen in the Re = 500 case. Furthermore, the amplitude of the oscillations increases as the flow

progresses downstream. Through the tenth wave, the oscillations are fundamentally periodic with a single dominant frequency, but further downstream, multiple frequencies are present in the signals. The instantaneous streamline plot in Figure 8 reflects the unsteady behavior triggered by instabilities in the flow.

Finally, at Re = 700, the flow is oscillatory beginning at the third wave, and once again, the oscillations are completely self-sustaining downstream of this point, with their amplitude increasing as the flow proceeds downstream. The time signals in Figure 9 exhibit patterns similar to those of the Re = 600 case. The flow is basically periodic with a single frequency through the eighth wave, but multiple frequencies are introduced downstream of this point. The instantaneous streamline plot in Figure 10 exhibits the multiple vortices and divergent core flow that result from the unsteady nature of the flow.

Time signals were also generated for the average friction factors and Nusselt numbers across each wavelength of the passage, as well as for the velocities at the probed locations. If the flow is unsteady, then the time signals for the average f and Nu values will be oscillatory, just as the velocity time signals are. However, these signals can be integrated to produce time-averaged values which are indicative of the average heat transfer and pressure drop within each wave of the passage. The time-averaged values for the friction factors and Nusselt numbers averaged across each wavelength are plotted in Figures 11 and 12, respectively, as a function of wave location relative to the inlet for all four Reynolds numbers investigated herein. Note that two sets of data are presented for Re = 500. One set of quantities was tabulated during the time the flow was steady, and the other set was obtained while it was unsteady.

Figure 11 shows that $\overline{f_{avg}}$ peaks at the second wave from the inlet, and then decreases monotonically down the passage. This is due to the developing nature of the flow. Near the beginning of the channel, the friction factor is higher for the lower Reynolds number cases than for the higher ones. However, it also decreases more rapidly at low Reynolds numbers, so that by the end of this 14-wave passage, the friction factor is higher for the higher Reynolds numbers.

Figure 12 clearly reveals how unsteady flow in a wavy channel can enhance heat transfer, while steady flow in the same geometry produces only minimal benefits. For Re = 300, and the steady flow at Re = 500, the Nusselt number remains virtually constant throughout the passage, beginning at the second wave from the inlet. The increase in the fourteenth wave for the Re = 500 case is due to the fact that in this wave, the flow is still oscillatory even during the time the flow is "steady". However, these oscillations are very small compared with those which occur when the flow is fully unsteady. For steady flow at these two Reynolds numbers, the values of $\overline{Nu_{avg}}$ are not that much greater than the Nu = 7.54 yielded by a straight channel. When the flow is unsteady at Re = 500, though, the Nusselt number rises significantly beginning in the eighth wave, where the flow becomes unsteady. At Re = 600, in the portion of the passage where the flow is steady, the Nusselt number remains constant from wave to wave, and is only slightly higher than for steady flow at Re = 500. However, once the flow becomes unsteady, beginning around the fifth wave, the value of $\overline{Nu_{avg}}$ begins to increase dramatically as the flow travels downstream. This rate of increase becomes even greater once the oscillations begin exhibiting dramatically increased amplitudes accompanied by multiple frequencies, around the twelfth wave. By the end of the wavy passage, the time-averaged Nusselt number has reached a value that is more than twice as large as the value in the waves near the inlet where the flow is completely steady. At Re = 700, the Nu plot is similar to that for Re = 600, but unsteadiness in the flow is present as far back as the third wave, and the values of Nu are even higher throughout the passage.

4. SUMMARY

Flow patterns in the developing portion of a sinusoidally curved converging-diverging channel have been investigated through accurate numerical solutions of the governing equations on a curvilinear orthogonal grid. The wavy channel studied corresponds to the geometry of Nishimura, et al. (1984). For Reynolds numbers less than 400, more than fourteen waves are needed for the flow instabilities to develop. At Re = 500, the flow becomes unsteady beginning at the eighth wave downstream from the inlet. Furthermore, the unsteadiness is observed to be intermittent. For Re = 600, completely self-sustaining oscillations are evident as far upstream as the fifth wave, and at Re = 700, the unsteady behavior is present in the third wave. Also, the overall length of the channel does not affect these locations of onset to unsteadiness. Information about the developing section of the channel is important, because effective enhancement of heat and mass transfer in a wavy passage can only be realized when the flow is unsteady.

REFERENCES

Greiner, M., Chen, R.-F. and Wirtz, R. A. (1990). "Heat Transfer Augmentation Through Wall-Shape-Induced Flow Destabilization." ASME Journal of Heat Transfer **112**(May), 336-341.

Guzmán, A. M. and Amon, C. H. (1994). "Transition to Chaos in Converging-Diverging Channel Flows: Ruelle-Takens-Newhouse Scenario." Physics of Fluids **6**(6), 1994-2002.

Mendes, P. S. and Sparrow, E. M. (1984). "Periodically Converging-Diverging Tubes and their Turbulent Heat Transfer, Pressure Drop, Fluid Flow, and Enhancement Characteristics." Transactions of the ASME, Journal of Heat Transfer **106**(February), 55-63.

Nishimura, T., Kajimoto, Y. and Kawamura, Y. (1986). "Mass Transfer Enhancement in Channels with a Wavy Wall." Journal of Chemical Engineering of Japan **19**(No. 2), 142-144.

Nishimura, T., Ohori, Y. and Kawamura, Y. (1984). "Flow Characteristics in a Channel With Symmetric Wavy Wall for Steady Flow." Journal of Chemical Engineering of Japan **17**(5), 466-471.

Sparrow, E. M. and Prata, A. T. (1983). "Numerical Solutions for Laminar Flow and Heat Transfer in a Periodically Converging-Diverging Tube, with Experimental Confirmation." Numerical Heat Transfer **6**, 441-461.

Wang, G. and Vanka, S. P. (1995). "Convective Heat Transfer in Periodic Wavy Passages." International Journal of Heat and Mass Transfer, **38**(No. 17), 3219-3230

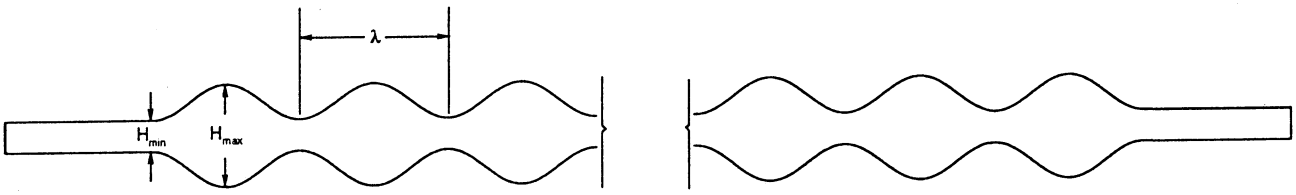

Fig. 1 Geometry of sinusoidal wavy channel

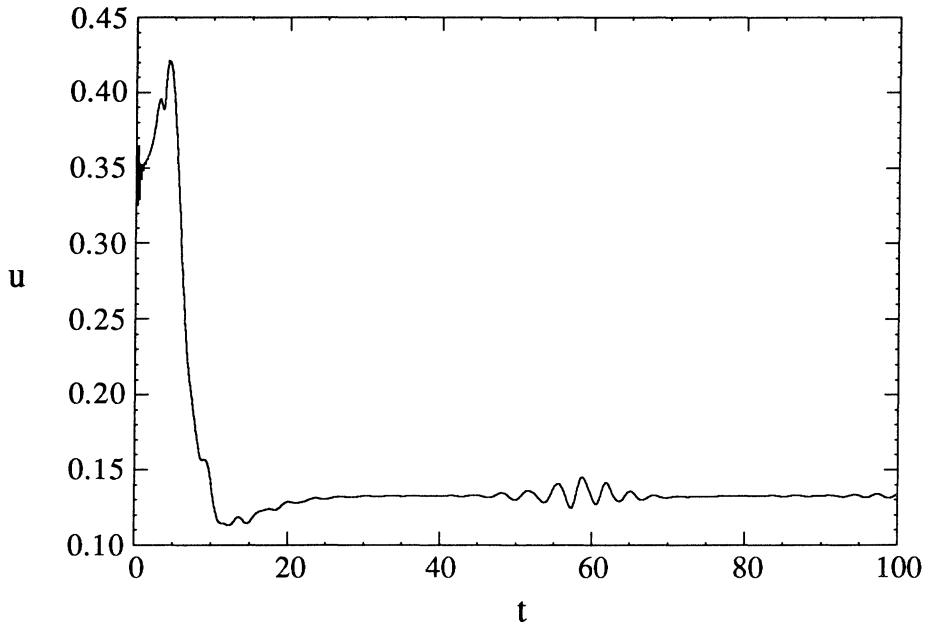

Fig. 2 Time signal for u-velocity in 14th wave at Re = 300

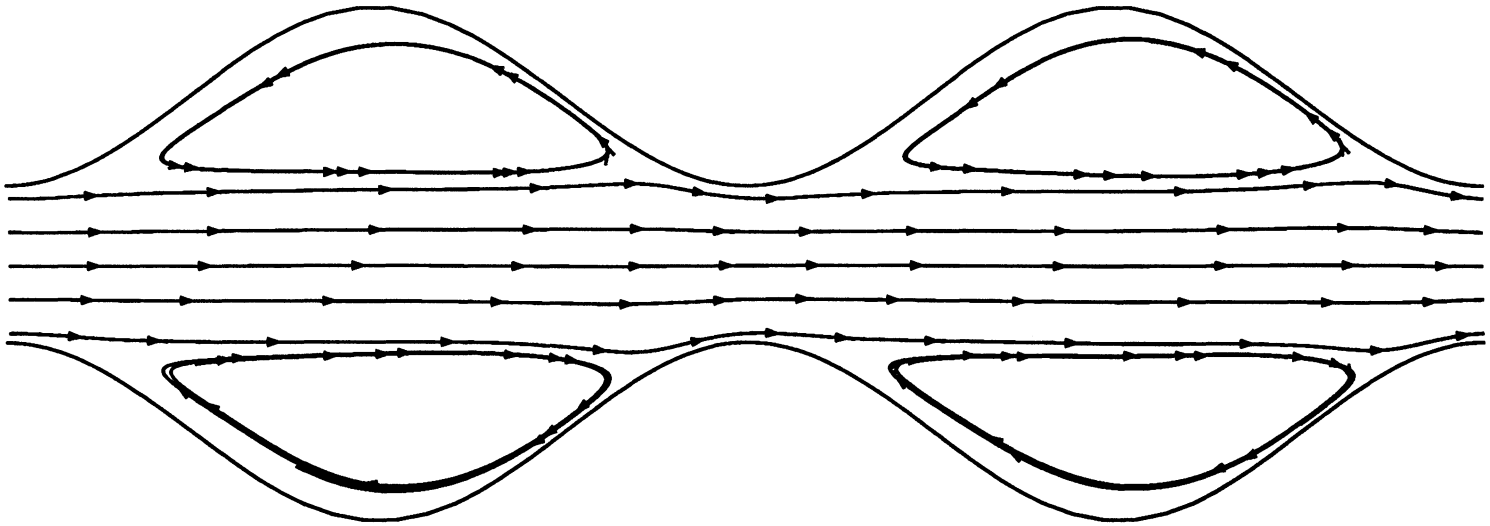

Fig. 3 Instantaneous streamline plot in 13th and 14th waves at Re = 300

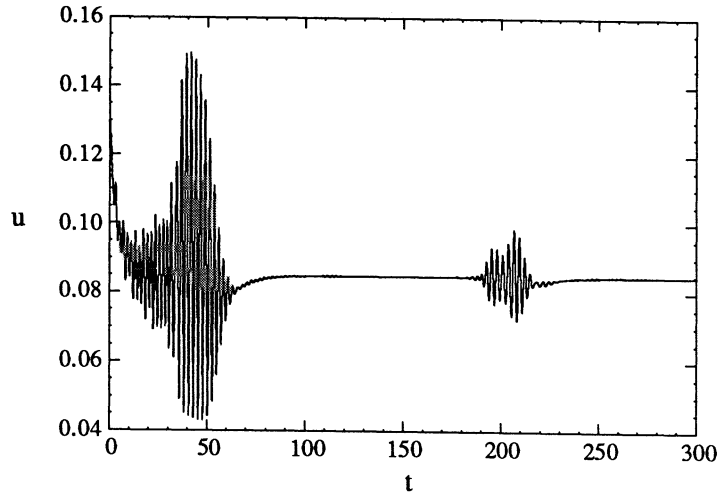

(a)

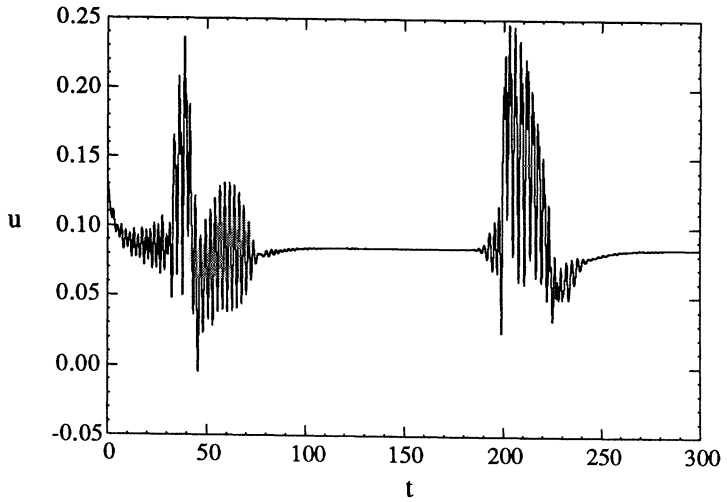

(b)

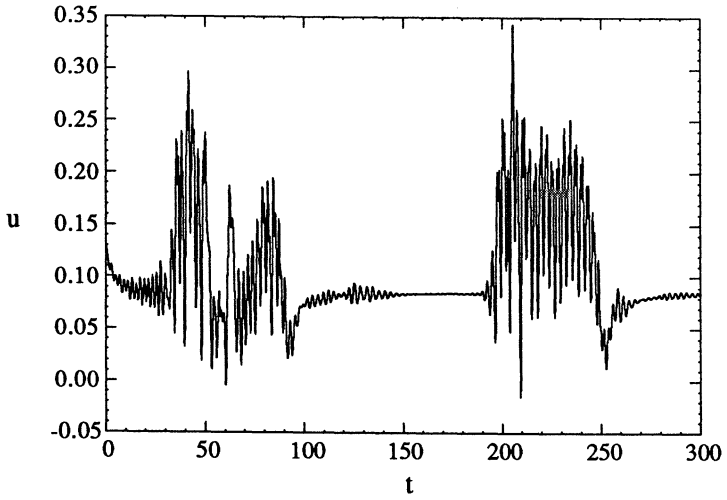

(c)

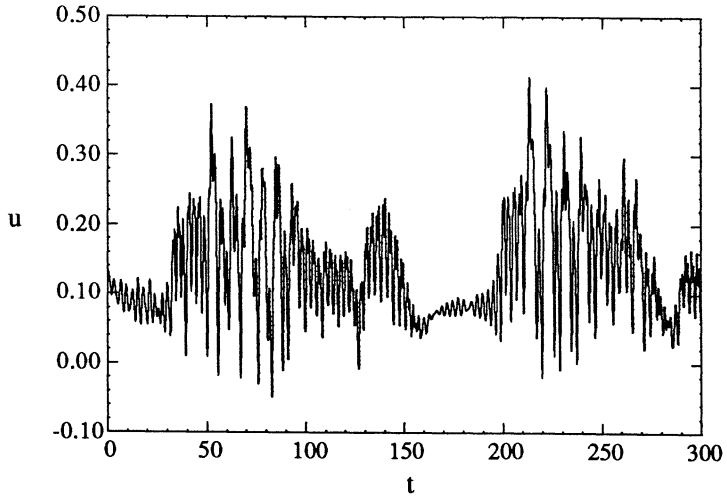

(d)

Fig. 4 Time Signals for u-velocity at Re = 500
(a) Wave 8, (b) Wave 10, (c) Wave 12, (d) Wave 14

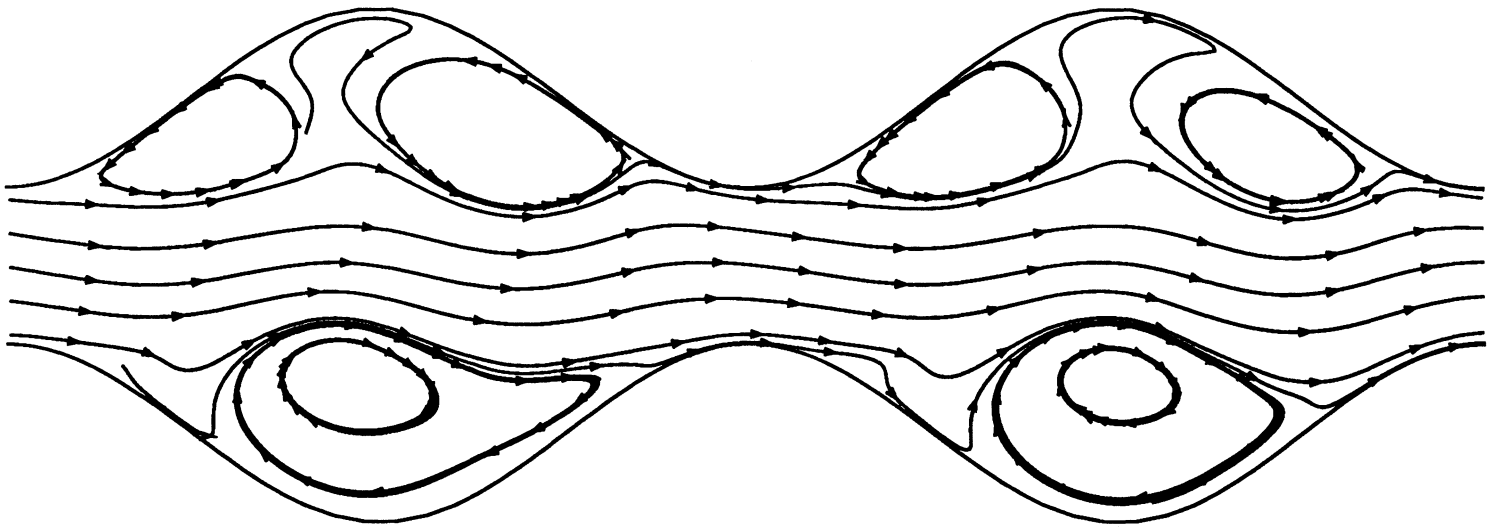

Fig. 5 Instantaneous streamline plot in 13th and 14th waves at Re = 500 (unsteady flow)

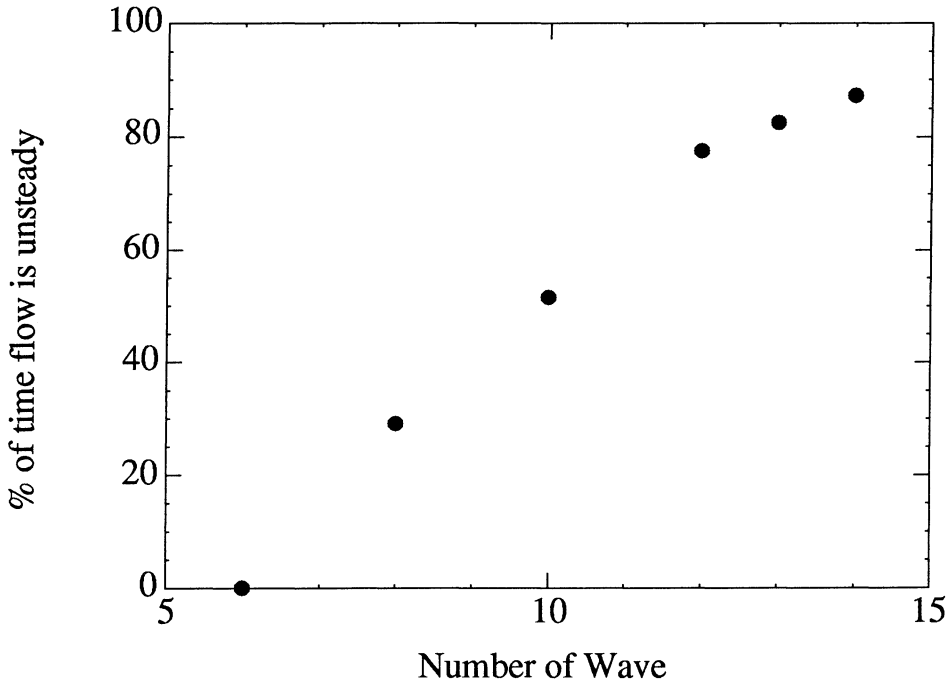

Fig. 6 Percentage of time flow is unsteady as a function of location at Re = 500

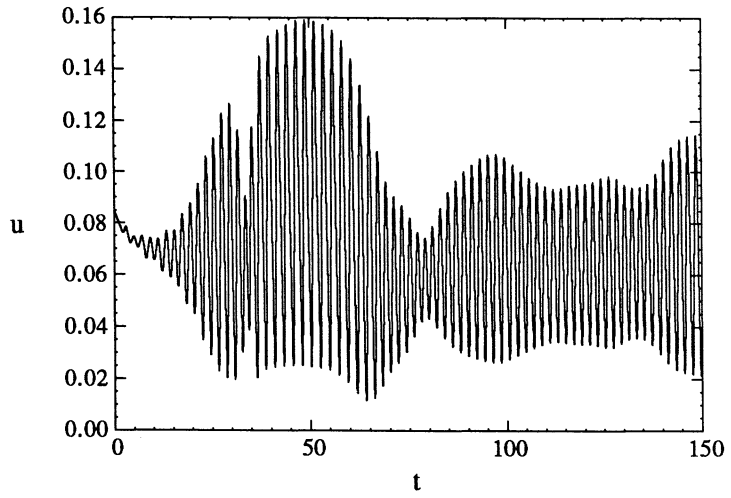

(a)

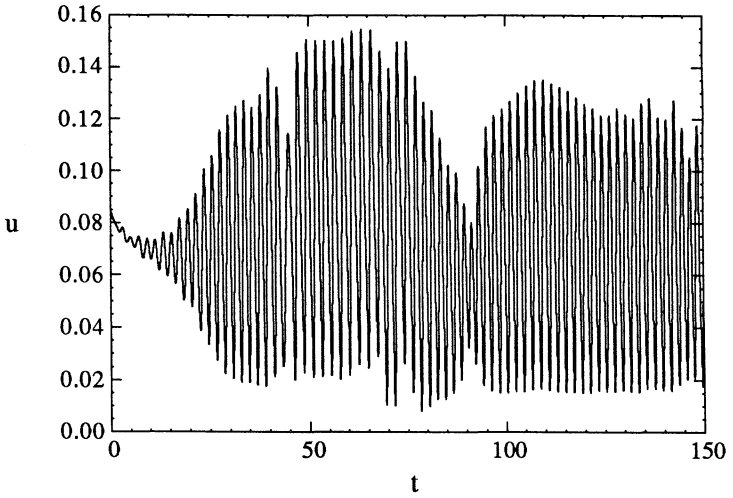

(b)

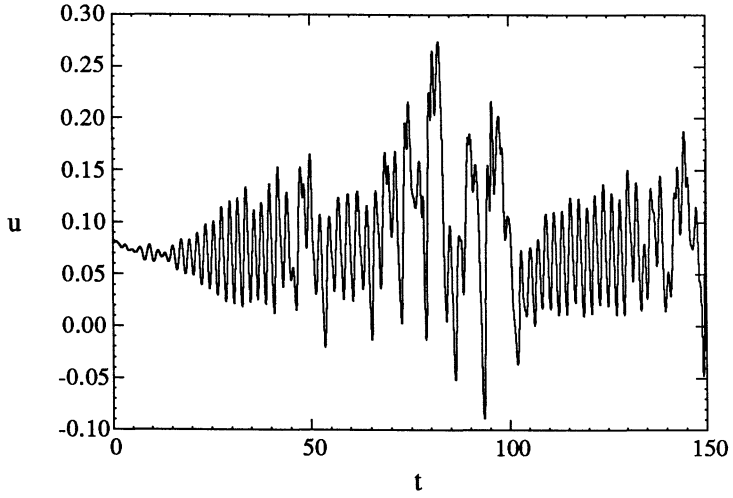

(c)

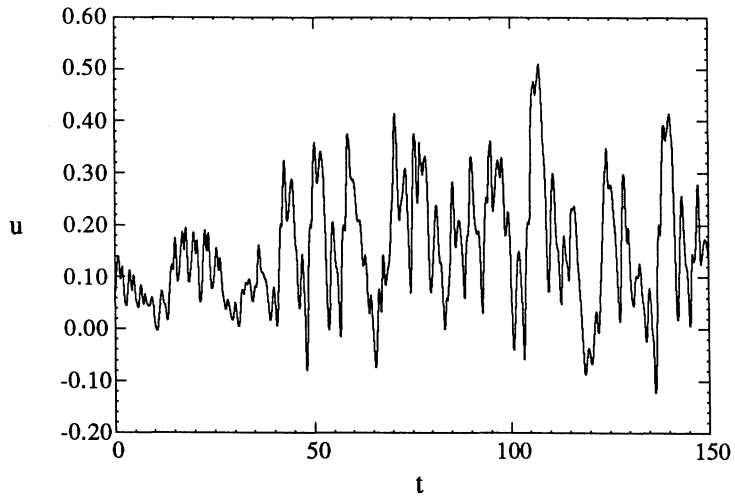

(d)

Fig. 7 Time Signals for u-velocity at Re = 600
(a) Wave 8, (b) Wave 10, (c) Wave 12, (d) Wave 14

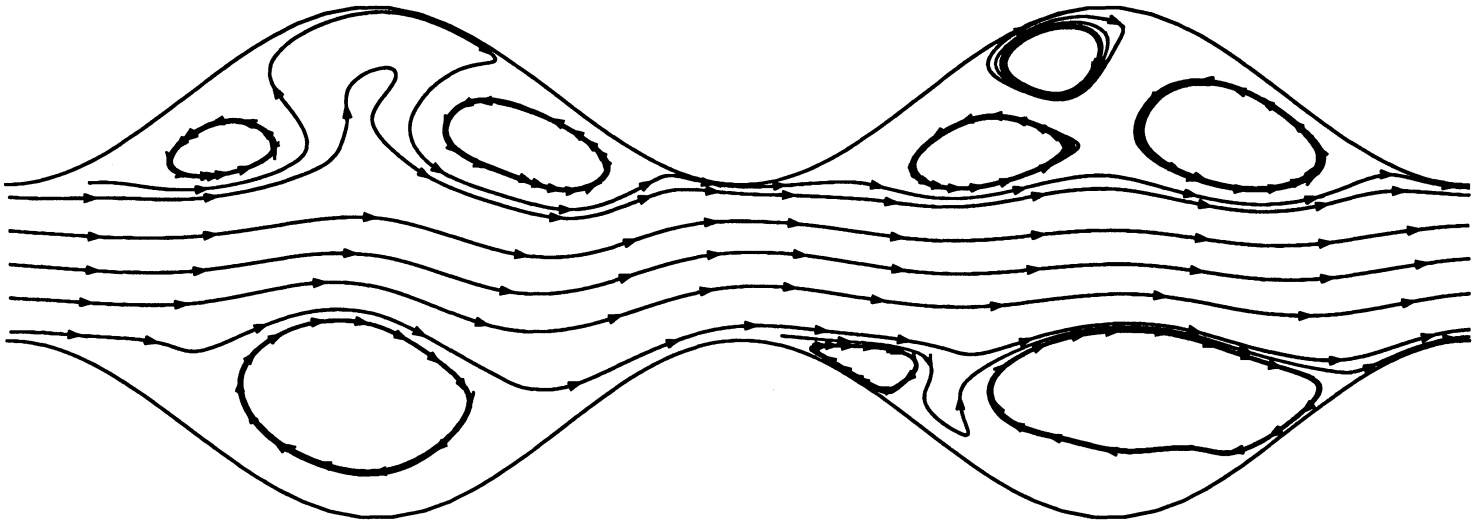

Fig. 8 Instantaneous streamline plot in 13th and 14th waves at Re = 600

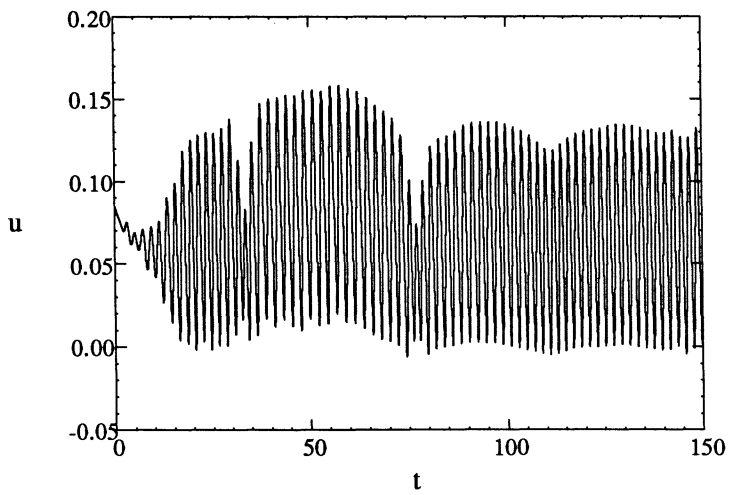

(a)

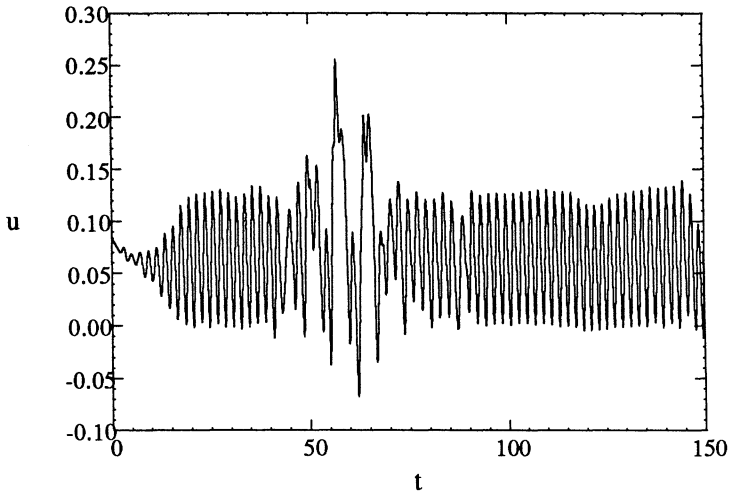

(b)

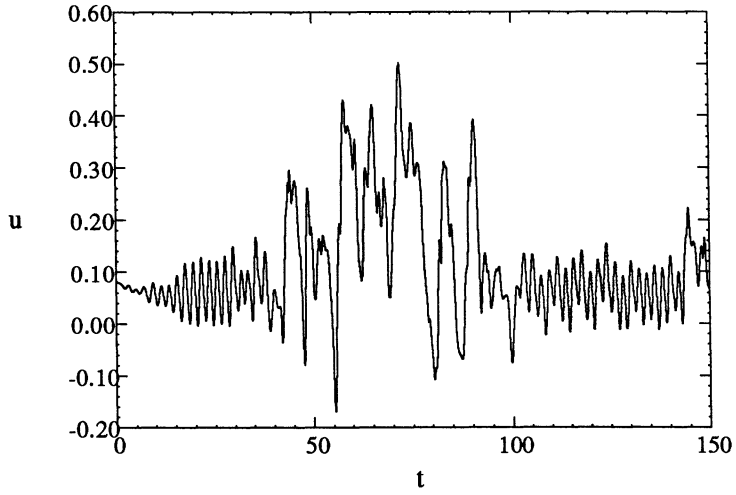

(c)

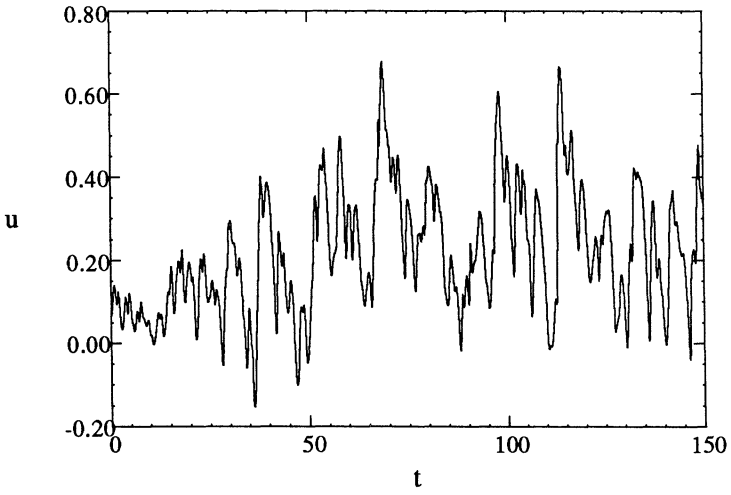

(d)

Fig. 9 Time Signals for u-velocity at Re = 700
(a) Wave 8, (b) Wave 10, (c) Wave 12, (d) Wave 14

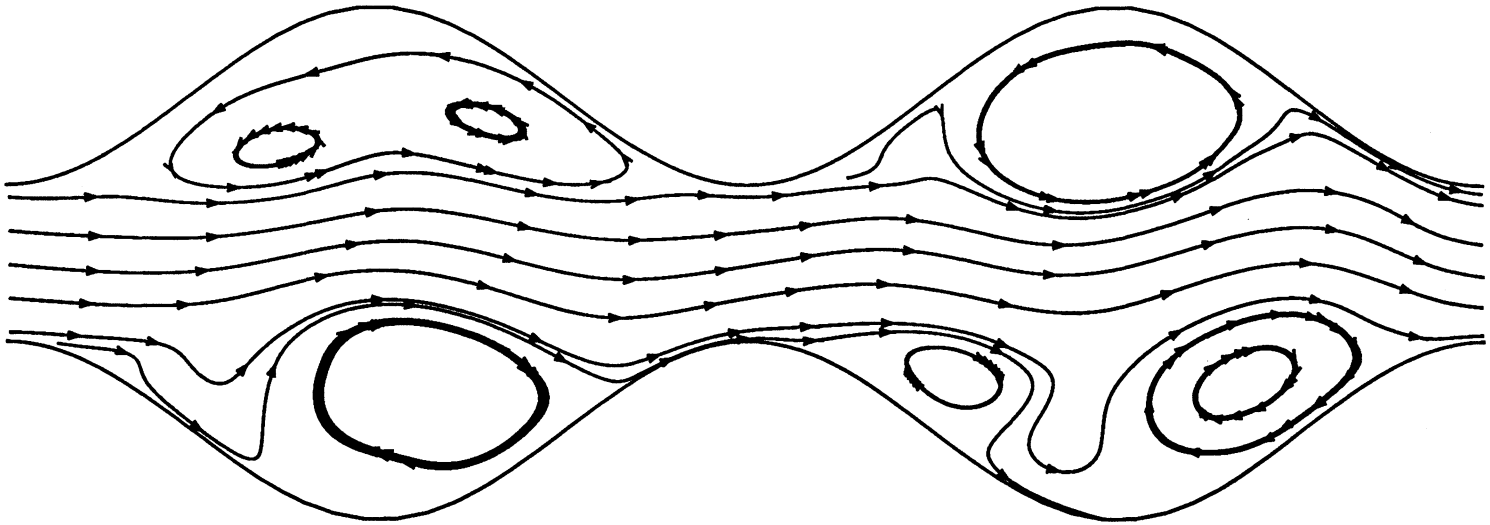

Fig. 10 Instantaneous streamline plot in 13th and 14th waves at Re = 700

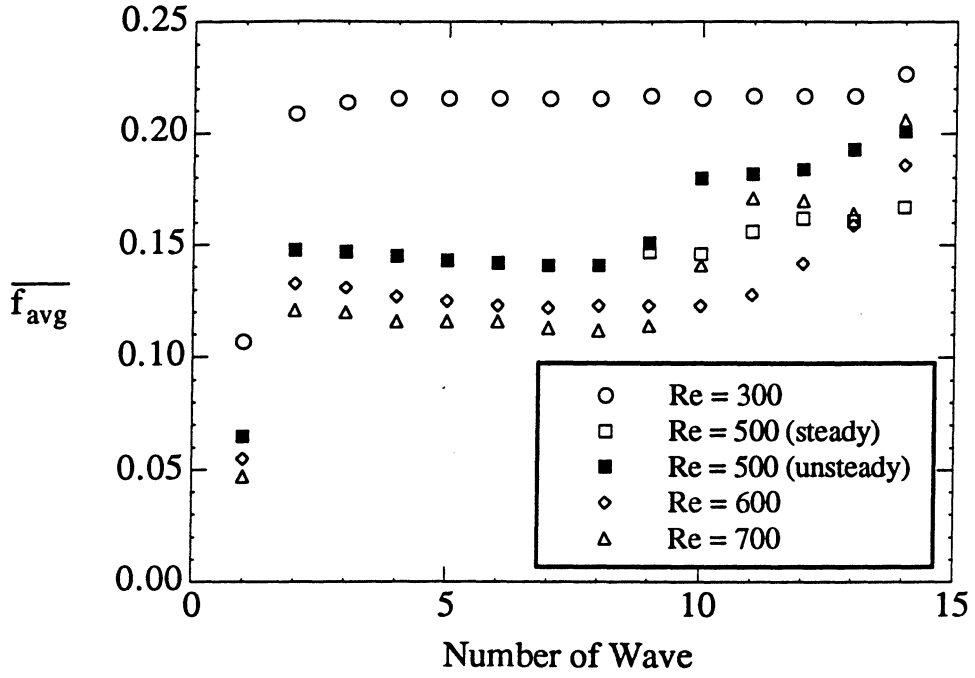

Fig. 11 Time-averaged friction factor averaged across each wavelength as a function of location

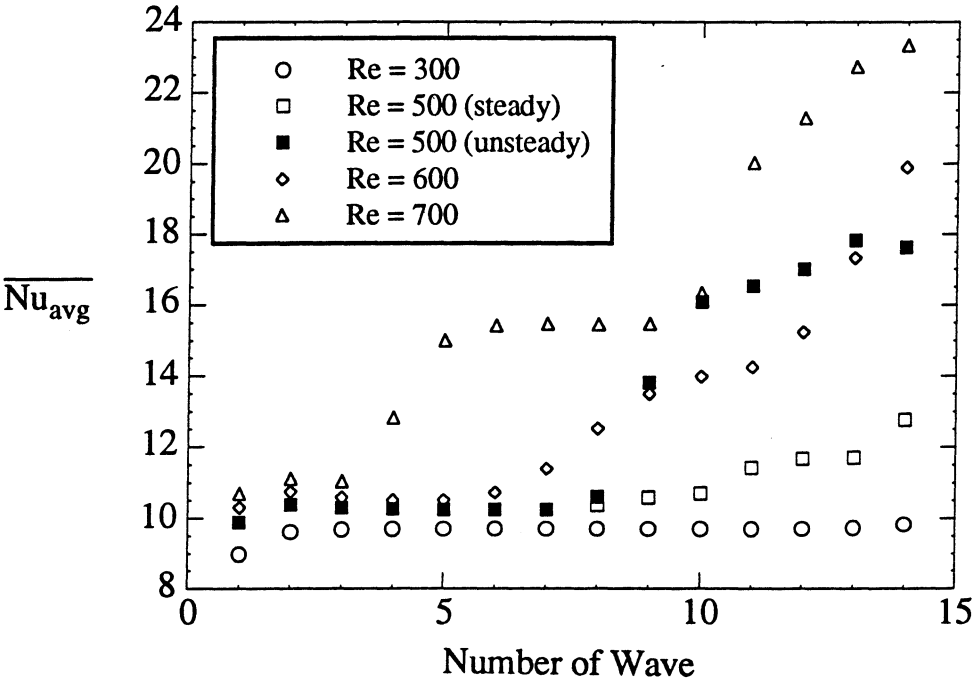

Fig. 12 Time-averaged Nusselt number averaged across each wavelength as a function of location